observed after about 3 days. Sols that were aged for at least 4 weeks were used for the electrical measurements.

Electrode arrays were created on silicon wafers with a 1 μm thick thermally grown oxide layer. Gold electrodes spaced by 3 μm were fabricated by conventional optical lithography. AuPd (40/60) lines with a separation of about 100 nm were defined by e-beam lithography using a two-layer resist and a modified Hitachi S2300 scanning electron microscope.

Before deposition of V_2O_5 fibers, the substrates were silanized for 2 min at room temperature by immersion in a 2.5 mM aqueous solution of 3-aminopropyltriethoxysilane (Aldrich), followed by thorough rinsing with pure water and drying under a stream of air.

V_2O_5 network samples were prepared as follows: A droplet of undiluted V_2O_5 sol, several days old, was deposited on the electrode structure with 3 μm gaps. After 15 min, the samples were rinsed with water and blown dry with air. For deposition of individual fibers on the electrode arrays or on bare substrates prior to e-beam lithography, the aminosilanized substrates were dipped into a mixture of V_2O_5 sol/water (1:10) for 2–3 s. The substrates were then rinsed with water and blown dry.

The samples were characterized with an SFM (Digital Instruments, Nanoscope IIIa) in tapping mode using conventional silicon cantilevers. The electrical transport measurements were performed under vacuum with a Keithley 617 electrometer and a Keithley 230 voltage source. The samples showed stable transport characteristics over several days.

Received: September 22, 1999
Final version: December 14, 1999

[1] S. Frank, P. Poncharal, Z. L. Wang, W. A. de Heer, *Science* **1998**, *280*, 1744
[2] S. J. Tans, A. R. M. Verschueren, C. Dekker, *Nature* **1998**, *393*, 49.
[3] R. Martel, T. Schmidt, H. R. Shea, T. Hertel, P. Avouris, *Appl. Phys. Lett.* **1998**, *73*, 2447.
[4] R. Saito, G. Dresselhaus, M. S. Dresselhaus, *Physical Properties of Carbon Nanotubes*, Imperial College Press, London **1998**.
[5] H. T. Soh, C. F. Quate, A. F. Morpurgo, C. M. Marcus, J. Kong, H. Dai, *Appl. Phys. Lett.* **1999**, *75*, 627.
[6] R. Tenne, L. Margulius, M. Genut, G. Hodes, *Nature* **1992**, *360*, 444.
[7] M. Remškar, Z. Škraba, M. Regula, C. Ballif, R. Sanjinés, F. Lévy, *Adv. Mater.* **1998**, *10*, 246.
[8] Y. Q. Zhu, W. B. Hu, W. K. Hsu, M. Terrones, N. Grobert, T. Karali, H. Terrones, J. P. Hare, P. D. Townsend, H. W. Kroto, D. R. M. Walton, *Adv. Mater.* **1999**, *11*, 844.
[9] H.-W. Fink, C. Schönenberger, *Nature* **1999**, *398*, 407.
[10] M. E. Spahr, P. Bitterli, R. Nesper, M. Müller, F. Krumeich, H. U. Nissen, *Angew. Chem. Int. Ed.* **1998**, *37*, 1263.
[11] J. Livage, *Coord. Chem. Rev.* **1998**, *178–180*, 999.
[12] X. Commeinhes, P. Davidson, C. Bourgaux, J. Livage, *Adv. Mater.* **1997**, *9*, 900.
[13] C. Guestaux, J. Leaut, C. Virey, J. Vial, *US Patent 3 658 573*, **1972**.
[14] T. Yao, Y. Oka, N. Yamamoto, *Mater. Res. Bull.* **1992**, *27*, 669.
[15] J. K. Bailey, G. A. Pozarnsky, M. L. Mecartney, *J. Mater. Res.* **1992**, *7*, 2530.
[16] R. M. Abdel-Latif, *Physica B* **1998**, *254*, 273.
[17] J. Haemers, E. Baetens, J. Vennik, *Phys. Status Solidi A* **1973**, *20*, 381.
[18] M. G. Kanatzidis, C.-G. Wu, *J. Am. Chem. Soc.* **1989**, *111*, 4139.
[19] N. Gharbi, C. Sanchez, J. Livage, J. Lemerle, L. Néjem, J. Lefebvre, *Inorg. Chem.* **1982**, *21*, 2758.
[20] C. T. Gibson, G. S. Watson, S. Myhra, *Scanning Electron Microsc.* **1997**, *19*, 564.
[21] T. Allersma, R. Hakim, T. N. Kennedy, J. D. Mackenzie, *J. Chem. Phys.* **1967**, *46*, 154.
[22] F. P. Koffyberg, F. A. Benko, *Philos. Mag. B* **1978**, *38*, 357.
[23] J. Bullot, P. Cordier, O. Gallais, M. Gauthier, J. Livage, *J. Non-Cryst. Solids* **1984**, *68*, 123.
[24] J. Bullot, O. Gallais, M. Gauthier, J. Livage, *Appl. Phys. Lett.* **1980**, *36*, 986.
[25] J. Livage, *Chem. Mater.* **1991**, *3*, 578.
[26] N. F. Mott, *J. Non-Cryst. Solids* **1968**, *1*, 1.
[27] J. Nygård, D. H. Cobden, M. Bockrath, P. L. McEuen, P. E. Lindelof, *Appl. Phys. A* **1999**, *69*, 297.
[28] C.-G. Wu, D. C. DeGroot, H. O. Marcy, J. L. Schindler, C. R. Kannewurf, Y.-J. Liu, W. Hirpo, M. G. Kanatzidis, *Chem. Mater.* **1996**, *8*, 1992.
[29] S. Lu, L. Hou, F. Gan, *Adv. Mater.* **1997**, *9*, 244.
[30] L. Livage, F. Beteille, C. Roux, M. Chatry, P. Davidson, *Acta Mater.* **1998**, *46*, 743.

Constructive Nanolithography: Site-Defined Silver Self-Assembly on Nanoelectrochemically Patterned Monolayer Templates**

By *Rivka Maoz,* Eli Frydman, Sidney R. Cohen,* and *Jacob Sagiv**

Dedicated to Professor Günther Wulff on the occasion of his 65th birthday

We have recently reported on the possibility of achieving non-destructive surface patterning of a vinyl-terminated silane monolayer self-assembled on silicon, by the application of an electrical bias to a conducting atomic force microscope (AFM) tip operated in normal ambient conditions.[1] The tip-induced transformation was shown to proceed by local electrochemical oxidation of the top vinyl functions of the monolayer, with full preservation of its overall molecular order and structural integrity. It was further shown that such nanoelectrochemically patterned monolayers may be employed as extremely robust, stable templates for the controlled self-assembly of organic bilayer structures with predefined size, shape, and surface location.[1]

Here we show that this template-controlled self-assembly strategy, referred to as *constructive nanolithography,* can be extended to the planned construction of hybrid metal–organic surface nanostructures. Starting with a thiol-top-functionalized silane monolayer (TFSM) with silver ions chemisorbed on its outer surface (Ag^+–TFSM), metallic silver nanoparticles are generated at selected surface sites by either wet chemical or tip-induced electrochemical reduction of the surface-bound metal ions. As illustrated in Figure 1, the conventional wet chemical reduction (e.g., with aqueous $NaBH_4$) can be used to cover macroscopic surface areas, with lateral dimensions from about 0.5 mm[2] to several centimeters, whereas site-defined reduction of the silver thiolate in the micron- down to the nanometer-size range can be achieved with the help of a conducting AFM tip. If desired, larger metal islands and thicker films, useful as electrical contacts and current leads, may be grown by further chemical development of the initially-generated silver particles (Fig. 1). Thus, silver metal structures are assembled according to a predefined design, by non-destructively im-

[*] Dr. R. Maoz, E. Frydman, Prof. J. Sagiv
Department of Materials and Interfaces
The Weizmann Institute of Science
76100 Rehovot (Israel)
Dr. S. R. Cohen
Chemical Services Unit
The Weizmann Institute of Science
76100 Rehovot (Israel)

[**] We are grateful to Dr. Kazufumi Ogawa of Matsushita Electric Industrial Co. (Osaka) for supplying the NTS used in the assembly of the monolayer templates. Support of this research by the MINERVA Foundation, Germany, the "G.M.J. Schmidt Minerva Center on Supramolecular Architectures", and an Eshkol fellowship (EF), Ministry of Science, Jerusalem, are acknowledged.

  0935-9648/00/0603-0424 $ 17.50+.50/0

ADVANCED MATERIALS

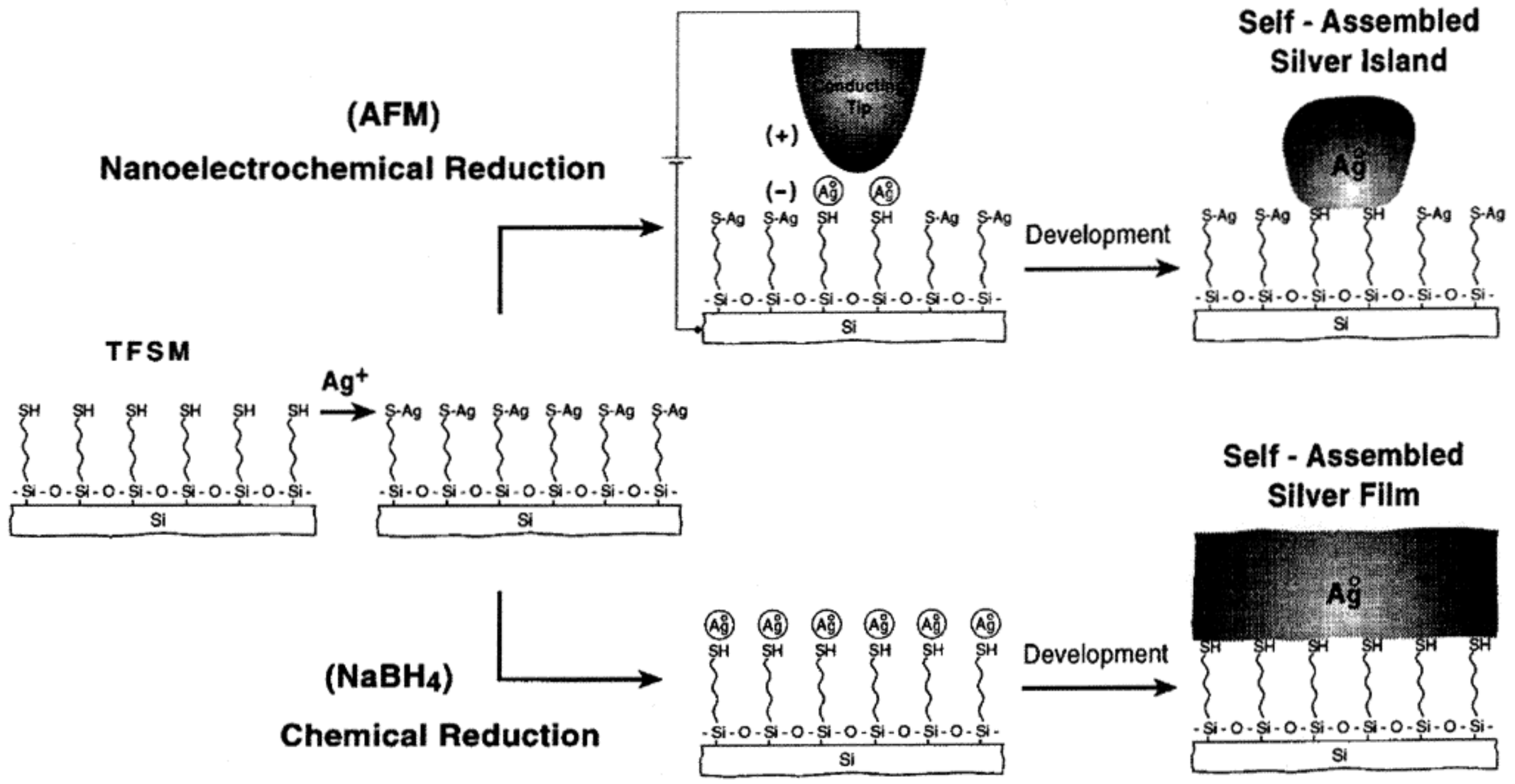

Fig. 1. Scheme of the site-defined self-assembly of silver metal on a thiol-top-functionalized silane monolayer (TFSM) preassembled on silicon (see text). The silver-thiolate (–S–Ag) template surface obtained by the chemisorption of Ag^+ ions on the TFSM surface (left side) is non-destructively patterned using either a wet chemical reduction process (lower path) or a nanoelectrochemical process (upper path) involving the application of a DC voltage to a conducting AFM tip (see Experimental), the slightly conducting silicon substrate being biased negatively (reductive bias) with respect to the tip. Further development of the macro- and, nano-patterns of reduced silver particles imprinted on the Ag^+–TFSM template (see Experimental) is shown to result in a thicker self-assembled silver film (lower path), or self-assembled silver islands selectively grown at tip-defined sites (upper path).

printing chemical information on the outer surface of a stable, solid supported organic monolayer that performs the function of an active template for spatial control of the metal self-assembly. As in the site-defined bilayer self-assembly demonstrated before,[1] once an initial pattern is inscribed on the outer surface of the base monolayer template, all subsequent operations leading to the final desired surface structure consist of in situ chemical modifications and self-assembly processes only, the monolayer template being preserved as an integral part of the resulting final structure. Thus, unlike lithographic methods based on resist removal and etch pattern-transfer technologies,[3] constructive nanolithography takes advantage of surface self-assembly processes that, by their very nature, hold promise for attractive new developments in nanofabrication, both in terms of the combined chemical-architectural diversity they offer and ultimate achievable miniaturization, beyond the inherent limits of the primary pattern inscription step. For example, as shown in the following, processes of spatially-confined self-assembly can be utilized to generate monolayer-bound metal particles (at tip-inscribed sites) significantly smaller than the effective size of the AFM tip used for patterning.

Densely packed, defect-free, TFSMs with variable surface concentrations of sulfur were produced photochemically[4] from high quality NTS precursor monolayers (NTS, 18-nonadecenyltrichlorosilane, $CH_2{=}CH{-}(CH_2)_{17}{-}SiCl_3$)[1], and NTS+OTS mixed monolayers (OTS, *n*-octadecyltrichlorosilane, $CH_3{-}(CH_2)_{17}{-}SiCl_3$)[4] self-assembled on slightly conducting silicon wafer substrates similar to those reported before[1] (see Experimental). Most of the present work was done on mixed monolayers with a molar ratio NTS/OTS = 1/2, which combine two desirable properties: a sufficiently large surface density of the sulfur-containing functions (generated from the terminal vinyl groups of NTS), together with enhanced surface hydrophobicity (due to the large percentage of outer CH_3 groups contributed by OTS).[5] The relatively high hydrophobicity of such monolayers permits easy handling of the wet chemical surface treatments and facilitates lateral confinement of the chemical reduction process, by the use of well-defined non-spreading droplets of the liquid reagents.[5] In-situ top-functionalized monolayers obtained by this method usually expose both thiol and disulfide surface functions, the formation of the latter depending on the packing density of the top vinyl groups in the precursor monolayer.[4] Considering the comparable silver-binding performance of the thiol and the disulfide,[4] no attempt was made deliberately to control the exact content of these functions in the different sulfur-containing monolayers examined during this study.[6] For brevity, we use here the term TFSM in a general sense, although the actual percentage of thiol groups in different TFSMs may vary, depending on the NTS/OTS molar ratios of the respective precursor monolayers.

The formation of nanoparticles of metallic silver + free thiol groups upon the wet chemical reduction of silver-thiolate monolayer surface groups (carried out over macroscopic surface areas; Fig. 1, lower path) was confirmed by UV-Vis spectroscopy, X-ray photoelectron spectroscopy

  0935-9648/00/0603-0425 $ 17.50+.50/0

ADVANCED MATERIALS

Using wet chemical reduction (Fig. 1, lower path), millimeter-size conducting silver electrodes could be produced within minutes on Ag^+–TFSM surfaces by a very simple procedure consisting of sequential placement and removal (with a pipette) of small drops of the reducing solution, pure water, the silver enhancer solution, and again pure water (see Experimental). The silver metal deposition was found to be well-defined by the position and size of each reducing drop, no metal film formation being observed outside the circumference of the corresponding reduced surface spots. The chemical and nanoelectrochemical processes (Fig. 1, lower and upper paths, respectively) can be easily combined, which may be particularly useful for the fabrication of electrical contacts between the macroscopic world and a self-assembled nanocircuit. This is demonstrated, for example, by the successful tip-induced generation of two silver islands at preselected surface sites near the edge of a conducting silver electrode fabricated by the wet chemical procedure described above (Fig. 2). It is of interest to note in Figure 2 the sharp edge of the electrode and the fact that silver metal was selectively deposited only within those areas of the Ag^+–TFSM template that were either exposed to the chemical reducing reagent or scanned with the tip under appropriate reductive bias prior to the application of the enhancer solution, despite the presence of Ag^+ ions on the entire imaged surface. This points to the equivalence of the chemical and tip-induced processes, the formation of reduced silver grains being effectively confined to those surface sites deliberately marked with the biased tip during the initial patterning step.

For many applications, it would be advantageous to be able to sequentially add new elements to a growing nanostructure, while continuously monitoring the entire build-up process with the help of a non-destructive inspection tool. Constructive nanolithography offers this option, as illustrated by the site-defined self-assembly, in six separate steps, of an array of nine silver islands (Fig. 3), using the nanoelectrochemical reduction and development process depicted in Figure 1. In the example given in Figure 3, individual islands as well as a pair of islands (step 4) were added sequentially to an initial set of three islands, the resulting structure being in-situ imaged (with the same conductive diamond tip used for patterning) before and after each of the operations involved in its construction. To demonstrate the flexibility of this self-assembly approach, the last added two islands (steps 5 and 6) were intentionally made much smaller than the first seven, with heights below 50 nm and lateral dimensions below about 0.4 μm. The successful implementation of such a sequence of site-defined metal deposition steps is obviously a consequence of the fact that no silver metal is deposited in the absence of intentional site activation by the tip, again pointing to the formation of metallic grains upon the reduction of surface-bound silver ions under the tip.

Examples of AFM images of primary (undeveloped) metal particles, generated by tip-induced nanoelectrochemical reduction of TFSM-bound silver ions, are given in Figure 4.[9] Image A shows clusters of nanoparticles with typical heights of 2–3 nm and lateral dimensions of the

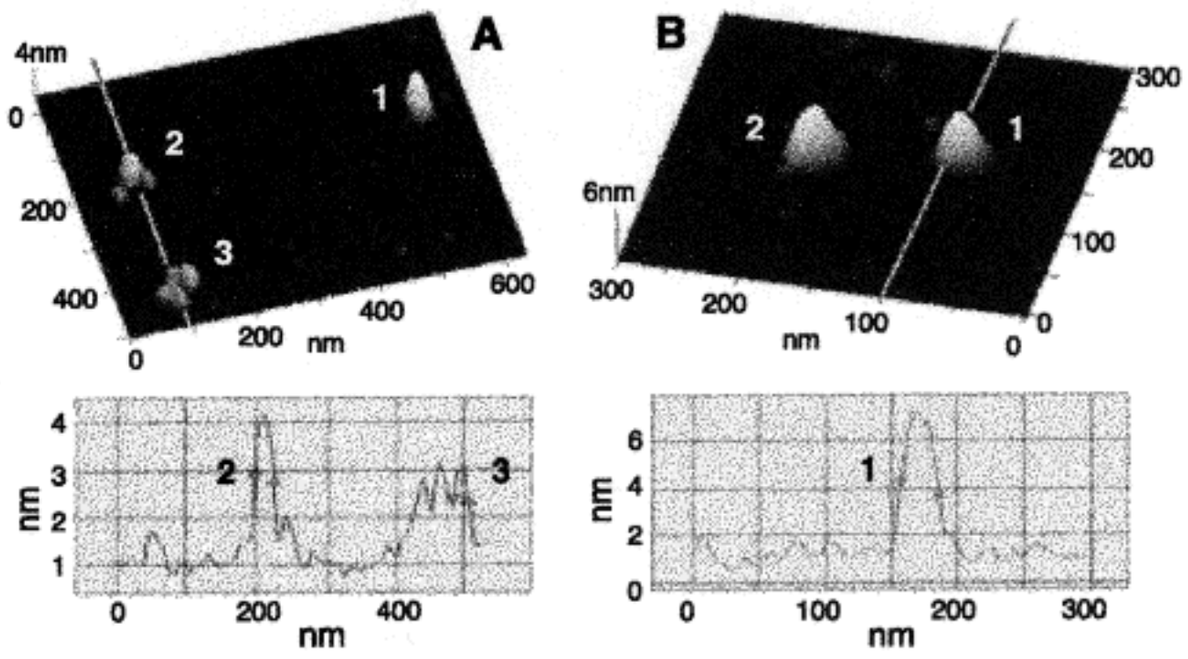

Fig. 4. Intermittent contact images (NT-MDT P47 instrument) of silver nanoparticles generated by tip-induced nanoelectrochemical patterning (according to Fig. 1, upper path without development) of a Ag^+–TFSM template as in Figure 2. The two images, A and B, consist of three and two discrete point features inscribed on the same monolayer surface, but with two different tips. The pattern inscription was done (in the contact mode) with reductive biases of 5–8 V between surface and tip and pulse lengths of 40–150 ms applied at each inscribed point (see Experimental). Characteristic particle dimensions are evident in the distance–height profiles (along the marked lines) shown below each image.

individual particles of 20–30 nm, while in B one can see isolated particles with heights of 5–6 nm and lateral dimensions of about 30 nm. Since these point features, in A and B, were produced on the same monolayer surface, but with different tips (also used for imaging), the resulting particles most probably reflect the interplay between tip size and shape[10] and the nucleation and growth kinetics of metal crystallites following the reduction of silver ions present within surface domains affected by the tip. It is thus interesting to note the formation of clustered metal particles, each particle having lateral dimensions 4–5 times smaller than those of the cluster itself (e.g., no. 3 in image A), that is, significantly smaller than the overall size of the tip-affected domain.

By analogy with the wet chemical reduction process, the selective deposition of silver metal from the silver enhancer solution at the tip-inscribed surface sites strongly suggests that, under the conditions of these experiments, the tip-induced transformation indeed involves local electrochemical reduction of the surface-bound Ag^+ ions to elemental silver. This view is confirmed by the results of a series of additional experiments, briefly summarized here, which provide further insight into the mechanism of the tip-induced Ag^+ reduction as well as into other possible modes of constructive nanolithography.

1) Upon treatment with the silver enhancer solution, no development was observed after the Ag^+–TFSM surface was scanned with a conducting diamond tip under reverse bias (i.e., tip negative, Si substrate positive). Likewise, a pattern "written" with a positively biased tip and then "rewritten" with the same tip negatively biased could not be developed. This implies that elemental silver generated in the reductive scanning mode undergoes oxidation when the

  0935-9648/00/0603-0427 $ 17.50+.50/0

(XPS), and AFM imaging,[4] while the structural stability of the template monolayers was routinely checked by taking quantitative Fourier transform infrared (FTIR) spectra of the investigated samples before and after each of the chemical operations indicated in Figure 1.[4] Silver nanoparticles generated by such wet chemical reduction of Ag^+–TFSM surfaces could be further developed (Fig. 1) using a silver self-assembly process that takes place exclusively around preformed silver metal nuclei, while being practically inactive at surface sites exposing unreduced silver ions only. In this manner, once a pattern of reduced silver is generated, further chemical deposition of silver metal would selectively amplify it, thus resulting in effective development of the initially inscribed chemical information (Fig. 1). This was realized by the application of a metal-catalyzed silver enhancer solution that deposits silver only on metal-seeded sites.[7,8] The rate of deposition and total amount of deposited silver were controlled by a number of adjustable parameters, such as the concentration of the enhancer solution and the time of contact with the activated surface (see Fig. 2 and Fig. 3). The selective development of silver metal grains upon treatment with the enhancer solution could thus be used as a sensitive indicator of the presence and location of reduced silver on the treated surface. This property was fully exploited in the nanoelectrochemical patterning experiments described in the following, for an unequivocal identification of tip-generated silver particles and their differentiation from grainy features originating in adventitious surface contamination, that may also show up in the AFM images.

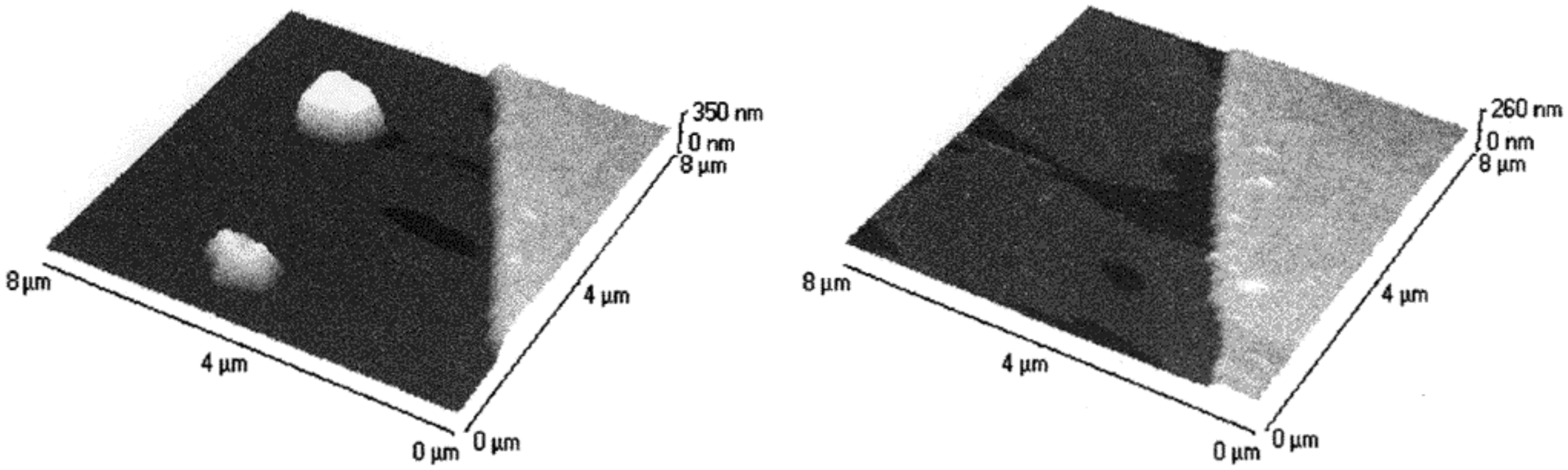

Fig. 2. Topographic contact-mode AFM images (Topometrix System) showing: (right side) portion of the edge of a millimeter-size silver electrode self-assembled on a Ag^+–TFSM template (made from a precursor mixed monolayer with a molar ratio NTS/OTS = 1/2; see text) by the wet chemical reduction and development process depicted in Figure 1, lower path (see text and Experimental); (left side) two self-assembled silver islands grown at tip-defined sites near the electrode edge shown in the image on the right, via the nanoelectrochemical reduction and development process depicted in Figure 1, upper path. The tip-induced reduction was done with a bias of +9.0 V (applied to the same diamond-coated tip used in imaging) and a scan speed of 2 µm s^{-1}. Compared to the development of the electrode (which was done with the original silver enhancer – see Experimental), the silver enhancer solution used in the development of the two islands was diluted by a factor of two and the time of contact with the surface reduced from 5 min to 2 min.

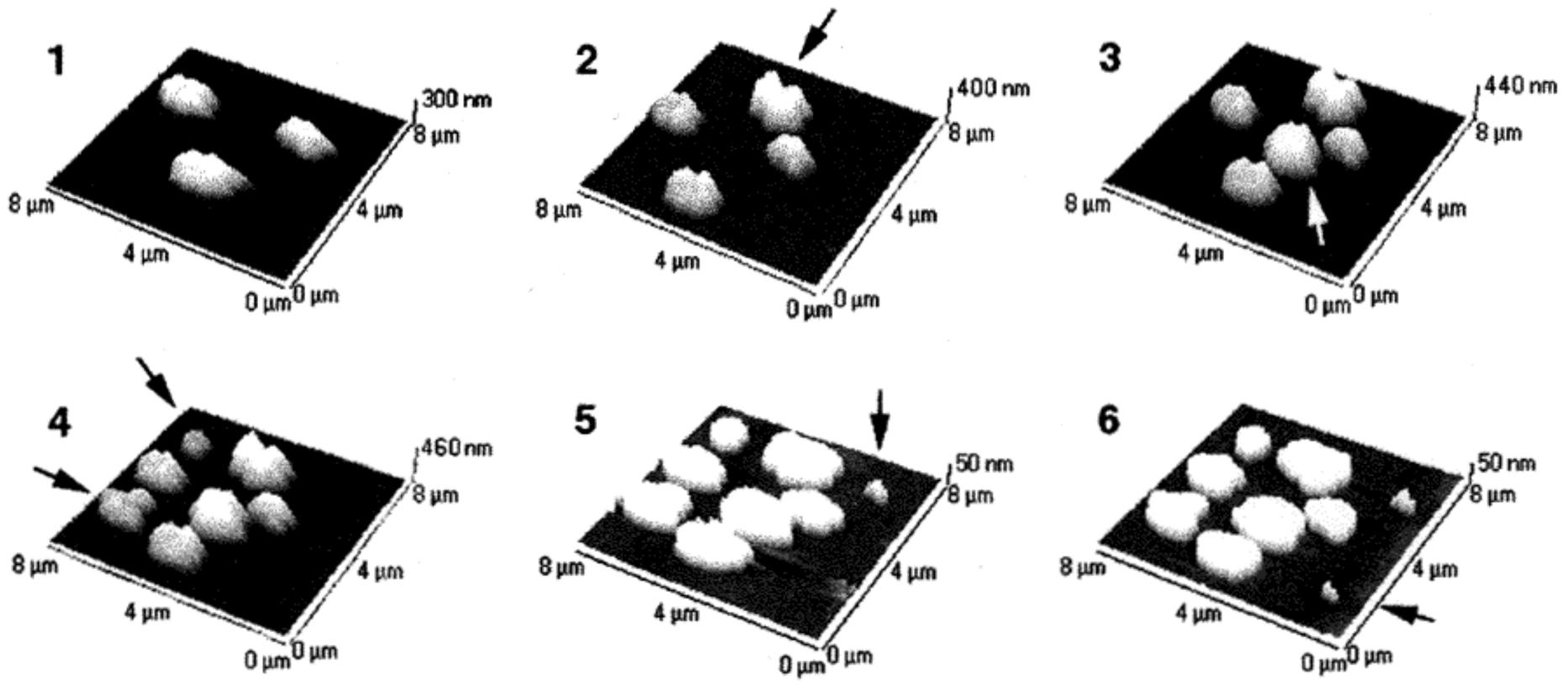

Fig. 3. AFM topographic record of the six successive steps during the fabrication of an array of nine silver islands at tip-defined sites on a Ag^+–TFSM template as in Figure 2 (using the lithographic process depicted in Fig. 1, upper path). Images were taken in the contact mode (Topometrix System), with the same diamond-coated tip employed in patterning, immediately after each development step (newly added islands are indicated by arrows). To facilitate easy visualization of the much smaller islands added in the last two steps, images 5 and 6 are presented with expanded *Z*-scales. The tip-induced Ag^+ reduction was done with a bias of +9.0 V (on the tip) and a scan speed of 2 µm s^{-1}, in steps 1 and 2, +10.0 V and 1.2 µm s^{-1} in step 3, and +10.0 V and 1 µm s^{-1} in steps 4–6. The concentration of the silver enhancer solution used for the development of the last two islands was lowered by a factor of 250 compared with that used for the other islands (for which the original enhancer solution was also diluted by a factor of two – see Experimental) and the time of contact with the surface reduced from 30 s to 15 s.

0935-9648/00/0603-0426 $ 17.50+.50/0

same scan is repeated in the oxidative mode. Scanning again the same area in the reductive mode (tip positive) enabled development, which implies reversibility of the oxidation process.

2) No development was found to occur when Ag^+–TFSM surfaces were scanned in an atmosphere of dry nitrogen, irrespective of the bias applied to the diamond tip. This clearly indicates that the tip-induced reduction of Ag^+–TFSMs, like the previously reported tip-induced oxidation of NTS monolayers,[1] is a water-mediated faradaic process[11] in which atmospheric water vapor condensing at the tip[12] plays an essential role.[13] The formation of elemental silver conceivably involves electrochemical reduction at the Ag^+–TFSM surface (cathode) and oxidation of water at the tip (anode):

at the surface (negative)

$$4R\text{–}S^-Ag^+ + 4e^- + 4H_2O \rightarrow 4R\text{–}SH + 4Ag^0 + 4OH^- \quad (1)$$

at the tip (positive)

$$2H_2O \rightarrow O_2 + 4H^+ + 4e^- \quad (2)$$

overall process

$$4R\text{–}S^-Ag^+ + 2H_2O \rightarrow 4R\text{–}SH + 4Ag^0 + O_2 \quad (3)$$

3) No deposition of silver from the silver enhancer solution was observed on a monolayer of OTS/Si or on bare silicon (after scanning with the diamond tip in the reductive mode), which confirms that no spurious surface processes, unrelated to the template-bound Ag^+ ions, could be responsible for the observed effects.

4) Finally, rather intriguing results were obtained when, in an attempt to locally deliver Ag^+ ions to a silver-free TFSM surface, the diamond-coated silicon tip was replaced with a silver-coated silicon nitride tip. In air, the reductive scanning mode (tip positive) produced a pattern that could not, however, be developed with the silver enhancer solution. On the other hand, development occurred when the reductive scanning was done under dry nitrogen. No effect was observed, either in air or in the dry nitrogen atmosphere, when the TFSM was scanned under reverse bias (tip negative) or without electrical bias. These observations can be rationalized if we assume that in humid air the positively biased silver tip (anode) is oxidized[11] and silver oxide or hydroxide particles rather than Ag^+ ions are released to the TFSM surface (cathode), where water is reduced:

at the tip (positive)

$$2Ag^0 + H_2O \rightarrow Ag_2O + 2H^+ + 2e^- \quad (4)$$

at the surface (negative)

$$2H_2O + 2e^- \rightarrow H_2 + 2OH^- \quad (5)$$

overall process

$$2Ag^0 + H_2O \rightarrow Ag_2O + H_2 \quad (6)$$

In dry nitrogen, a water-free electrochemical process occurs, whereby Ag^+ ions generated at the positive silver tip adsorb on the negative TFSM surface, where further rapid reduction to elemental silver occurs:

at the tip (positive)

$$Ag^0 \rightarrow Ag^+ + e^- \quad (7)$$

at the surface (negative)

$$R\text{–}SH + Ag^+ + e^- \rightarrow R\text{–}SH + Ag^0 \quad (8)$$

overall process

transfer of Ag^0 from tip to surface (9)

Taken together, the combined results of the present described "macro-" and "micro-size" experiments provide conclusive evidence for the feasibility of site-defined self-assembly of silver metal on both chemically and nanoelectrochemically patterned monolayer templates with sulfur-containing outer groups. Two modes of non-destructive patterning with electrically biased AFM tips were examined, both of which generate an initial, template-stabilized pattern of elemental silver grains, which can be further developed by treatment of the surface with a silver enhancer solution. In one mode, Ag^+ ions bound to the surface of the template are locally reduced with a silver-free conducting tip operating in normal ambient conditions, whereas in the second mode, elemental silver is locally transferred from a silver-coated tip to a silver-free template surface scanned under dry nitrogen. The available evidence suggests that a water-mediated faradaic mechanism is, most probably, operative in the first mode, whereas the second mode involves a dry electrochemical process facilitated by the direct contact between oppositely biased tip and template. The net result of the latter process may thus be regarded as representing electrically-driven transport of silver metal from the tip to a stable, silver-binding monolayer surface, the tip acting here as a nanometric solid-state "fountain-pen" that delivers a solid "ink" (silver metal) to a "paper" consisting of a functional surface with chemical affinity for this particular "ink".[14]

In conclusion, proof-of-concept experiments have been carried out demonstrating the possible utilization of constructive nanolithography as a versatile approach to the in situ chemical fabrication of spatially defined metal structures on organic monolayer templates. It was further shown that a simple change of experimental conditions, involving the tip material, the composition of the template surface, and the composition of the ambient atmosphere, may result in a different, yet useful mode of nanoelectrochemical surface patterning, which points to the versatility and wide applicability of the method.

While the present proof-of-concept study was not intended to explore the limits of miniaturization achievable by the described new approach, we should emphasize that, in principle, it offers attractive options for miniaturization

0935-9648/00/0603-0428 $ 17.50+.50/0

ADVANCED MATERIALS

beyond the smallest surface features that might be directly generated through the patterning process (Fig. 4A). This follows from the fact that a 3D object, such as a metal or semiconductor particle, grown from a sub-monolayer supply of surface-bound metal ions (available within a lithographically defined 2D monolayer domain with limited ion binding capacity), must necessarily be smaller than the domain itself. Relying on such processes of "laterally confined" self-assembly and growth rather than on etch and removal of material, constructive nanolithography is (unlike most other lithographic schemes) intrinsically adapted to transcend the limits of miniaturization inherent in the primary patterning process itself. This aspect, currently investigated by us, holds great promise for a series of future applications, particularly in nanoelectronics,[15] that are critically dependent on the ability to assemble and address complex functional structures with precisely defined nanometric dimensions.

Experimental

The precursor monolayers were prepared as described before [1], on double-sided polished p-type silicon wafer substrates (Semiconductor Processing Co., 0.5 mm thick, orientation <100>, resistivity 8–11 Ω cm). For the mixed monolayers, use was made of adsorption solutions with NTS/OTS molar ratios equal to the desired surface molar ratios [16]. The thiol/disulfide top functions were in situ introduced, through the photo-induced radical addition of H_2S to the terminal ethylenic double bond of NTS [4]. Adsorption of Ag^+ ions from a 10^{-3} M aqueous solution of silver acetate on the TFSM surfaces, followed by rinsing with pure water in order to remove surplus silver solution that may stick to the surface [4], finally completed the preparation of the Ag^+–TFSM templates.

Most nanopatterning experiments were carried out as before [1] (the surface being now negatively biased with respect to the tip) with a Topometrix TMX 2010 Discoverer system using boron-doped chemical vapor deposited (CVD) diamond-coated silicon probes [1] or silicon nitride probes that were coated with silver by metal evaporation. The images shown in Figures 2 and 3 were taken with the same probes (without electrical bias) in the contact mode, with minimal contact forces, typically 50 nN or less, including the inherent tip-surface attraction.

The pattern inscription and imaging of the features shown in Figure 4 were done on a NT-MDT P47 instrument. Probes were conductive W_2C-coated silicon tips (Silicon-MDT) with normal spring constants of 0.5–2 N/m, resonance frequencies of 60–180 kHz, and Q of 80–140. These characteristics allowed using the same probe in both contact and intermittent contact modes. The former was used for pattern inscription, and the latter (without electrical bias) for imaging [9]. Pattern inscription was carried out using the system software, which allows defining a dwell time and voltage bias for each point of the pattern. In order to produce small feature size, the features were written as single points. This could be done by holding the sample at ground potential and applying a positive pulse to the tip, or holding the tip at ground potential and applying a negative pulse to the sample. Except where otherwise mentioned, the entire AFM patterning and imaging work was done under normal ambient conditions (23–25 °C, 50–60 % relative humidity).

For the wet chemical Ag^+ reduction, drops of a 10^{-2} M aqueous solution of $NaBH_4$ were placed on the Ag^+–TFSM surface for about 2 min, then removed and the surface rinsed with drops of pure water. The development of the silver grains generated in the initial Ag^+ reduction step was accomplished with a commercial silver enhancer solution (Sigma, Silver Enhancer Kit) which was further diluted with pure water when lower metal deposition rates were desired [4]. Drops of the enhancer solution were placed on the template surface for the specified periods of time, then removed and the surface rinsed with drops of pure water. The removal of the drops was done by suction with a sharp pipette without any visible traces of liquid being left on the surface [5].

Received: April 29, 1999
Final version: November 29, 1999

[1] R. Maoz, S. R. Cohen, J. Sagiv, *Adv. Mater.* **1999**, *11*, 55.
[2] Micropipette delivery may allow targeting of the reducing solution to sub-micron surface areas.
[3] See, for example: a) N. Mino, S. Ozaki, K. Ogawa, M. Hatada, *Thin Solid Films* **1994**, *243*, 374. b) M. J. Lercel, H. G. Craighead, A. N. Parikh, K. Seshadri, D. L. Allara, *Appl. Phys. Lett.* **1996**, *68*, 1504. c) J. H. Thywissen, K. S. Johnson, R. Younkin, N. H. Dekker, K. K. Berggren, A. P. Chu, M. Prentiss, S. A. Lee, *J. Vac. Sci. Technol. B* **1997**, *15*, 2093. d) Y. Xia, G. M. Whitesides, *Angew. Chem. Int. Ed.* **1998**, *37*, 550. e) F. K. Perkins, E. Dobisz, S. L. Brandow, T. S. Koloski, J. M. Calvert, K. W. Rhee, J. E. Kosakowski, C. R. K. Marrian, *J. Vac. Sci. Technol. B* **1994**, *12*, 3725. f) J. K. Schoer, C. B. Ross, R. M. Crooks, T. S. Corbitt, M. J. Hampden-Smith, *Langmuir* **1994**, *10*, 615. g) H. Sugimura, K. Okiguchi, N. Nakagiri, M. Miyashita, *J. Vac. Sci. Technol. B* **1996**, *14*, 4140. h) D. C. Tully, K. Wilder, J. M. J. Fréchet, A. R. Trimble, C. F. Quate, *Adv. Mater.* **1999**, *11*, 314.
[4] a) E. Frydman, *Ph.D. Thesis*, Weizmann Institute, submitted September **1999**. b) E. Frydman, R. Maoz, J. Sagiv, unpublished.
[5] The water contact angles characteristic of TFSMs obtained from mixed precursor monolayers with a molar ratio NTS/OTS = 1/2 vary from about 70° (adv.) and 64° (rec.) on the silver-free surface, to about 67° (adv.; rec.) on the surface fully loaded with Ag^+ ions.
[6] Disulfide surface functions obtained as the primary main product of the photo-induced reaction of H_2S with pure NTS monolayers (see Experimental) may subsequently be converted to thiol groups by chemical reduction with a suitable reducing reagent [4].
[7] See, for example: a) H. Schmidt, *Histochemistry* **1981**, *71*, 89. b) G. Danscher, J. D. R. Nörgaard, *J. Hystochem. Cytochem.* **1983**, *31*, 1394. c) G. B. Birrel, D. L. Habilstone, K. K. Hedberg, O. H. Griffith, *J. Histochem. Cytochem.* **1986**, *34*, 339.
[8] E. Braun, Y. Eichen, U. Sivan, G. Ben-Yoseph, *Nature* **1998**, *391*, 775.
[9] Lateral smearing of the deposited metal was occasionally observed during AFM imaging in the contact mode, because of the strong lateral forces exerted by the tip in this mode. This effect was particularly detrimental in the imaging of the small particles generated during the initial nanoelectrochemical reduction step (Fig. 1, upper path). In order to obtain satisfactory images it was necessary to switch from the contact mode used in pattern inscription to imaging in the intermittent contact mode. This could be conveniently accomplished with an NT-MDT P47 instrument (see Fig. 4 and Experimental) purchased toward the final stages of the work reported in this communication.
[10] Because of the convolution with the tip, the measured lateral dimensions of the particles may be overestimated.
[11] F. Forouzan, A. J. Bard, *J. Phys. Chem. B* **1997**, *101*, 10876.
[12] R. D. Piner, C. A. Mirkin, *Langmuir* **1997**, *13*, 6864.
[13] H. Sugimura, N. Nakagiri, *J. Vac. Sci. Technol. A* **1996**, *14*, 1223.
[14] An analogous "inverted" process, referred to as "dip-pen" nanolithography, was recently reported, whereby a molecular "ink" made of monolayer-forming thiol molecules is mechanically delivered from a "ink-loaded" AFM tip acting as "pen" to a solid gold surface acting as "paper": R. D. Piner, J. Zhu, F. Xu, S. Hong, C. A. Mirkin, *Science* **1999**, *283*, 661.
[15] H. Ahmed, *J. Vac. Sci. Technol. B* **1997**, *15*, 2101.
[16] The NTS/OTS molar ratio on the surface was found (from quantitative FTIR spectra) to be practically identical to that of the adsorption solution used for the self-assembly of the mixed monolayer [4].

  0935-9648/00/0603-0429 $ 17.50+.50/0